Engineering selectivity into RGK GTPase inhibition of voltage-dependent calcium channels

Akil A. Puckerin[a,1], Donald D. Chang[b,1], Zunaira Shuja[b,1], Papiya Choudhury[b], Joachim Scholz[a,c], and Henry M. Colecraft[a,b,2]

[a]Department of Pharmacology and Molecular Signaling, College of Physicians and Surgeons, Columbia University, New York, NY 10032; [b]Department of Physiology and Cellular Biophysics, College of Physicians and Surgeons, Columbia University, New York, NY 10032; and [c]Department of Anesthesiology, College of Physicians and Surgeons, Columbia University, New York, NY 10032

Edited by Richard W. Aldrich, The University of Texas at Austin, Austin, TX, and approved October 8, 2018 (received for review June 28, 2018)

Genetically encoded inhibitors for voltage-dependent Ca^{2+} (Ca_V) channels (GECCIs) are useful research tools and potential therapeutics. Rad/Rem/Rem2/Gem (RGK) proteins are Ras-like G proteins that potently inhibit high voltage-activated (HVA) Ca^{2+} (Ca_V1/Ca_V2 family) channels, but their nonselectivity limits their potential applications. We hypothesized that nonselectivity of RGK inhibition derives from their binding to auxiliary $Ca_V\beta$-subunits. To investigate latent $Ca_V\beta$-independent components of inhibition, we coexpressed each RGK individually with Ca_V1 ($Ca_V1.2/Ca_V1.3$) or Ca_V2 ($Ca_V2.1/Ca_V2.2$) channels reconstituted in HEK293 cells with either wild-type (WT) β_{2a} or a mutant version ($\beta_{2a,TM}$) that does not bind RGKs. All four RGKs strongly inhibited Ca_V1/Ca_V2 channels reconstituted with WT β_{2a}. By contrast, when channels were reconstituted with $\beta_{2a,TM}$, Rem inhibited only $Ca_V1.2$, Rad selectively inhibited $Ca_V1.2$ and $Ca_V2.2$, while Gem and Rem2 were ineffective. We generated mutant RGKs (Rem[R200A/L227A] and Rad[R208A/L235A]) unable to bind WT $Ca_V\beta$, as confirmed by fluorescence resonance energy transfer. Rem[R200A/L227A] selectively blocked reconstituted $Ca_V1.2$ while Rad[R208A/L235A] inhibited $Ca_V1.2/Ca_V2.2$ but not $Ca_V1.3/Ca_V2.1$. Rem[R200A/L227A] and Rad[R208A/L235A] both suppressed endogenous $Ca_V1.2$ channels in ventricular cardiomyocytes and selectively blocked 25 and 62%, respectively, of HVA currents in somatosensory neurons of the dorsal root ganglion, corresponding to their distinctive selectivity for $Ca_V1.2$ and $Ca_V1.2/Ca_V2.2$ channels. Thus, we have exploited latent β-binding–independent Rem and Rad inhibition of specific Ca_V1/Ca_V2 channels to develop selective GECCIs with properties unmatched by current small-molecule Ca_V channel blockers.

Ca_V channel | RGK GTPase | channel inhibition | calcium channel | calcium channel gating

High voltage-activated (HVA) Ca^{2+} (Ca_V) channels convert electrical signals into Ca^{2+} influx that controls myriad essential processes including neuronal communication, muscle contraction, hormone release, and activity-dependent gene transcription (1). HVA Ca_V channels are composed of a pore-forming α_1- assembled with auxiliary β-, $\alpha_2\delta$-, and γ-subunits and calmodulin. There are seven α_1-subunits ($Ca_V1.1$ to 1.4 and $Ca_V2.1$ to 2.3), four $Ca_V\beta$s (β_1 to β_4), and three $\alpha_2\delta$s ($\alpha_2\delta1$ to $\alpha_2\delta3$), each with multiple splice variants. $Ca_V\alpha_1$-subunits contain the voltage sensor, selectivity filter, and channel pore, while auxiliary subunits regulate channel properties—$Ca_V\beta$s are obligatory for α_1-trafficking to the plasma membrane and for modulating channel gating (2); $\alpha_2\delta$s enhance channel surface trafficking and also modulate channel gating (3); and calmodulin promotes channel trafficking, enhances basal open probability (P_o), and confers feedback Ca^{2+} regulation of channel gating (4, 5).

Ca_V channels are also regulated by various intracellular signaling proteins and posttranslational modifications as a mechanism to control physiology. Pharmacological blockade of Ca_V1/Ca_V2 channels is an important treatment strategy for diverse diseases including hypertension, cardiac arrhythmias, chronic pain, and Parkinson's disease (1). RGK proteins (Gem, Rad, Rem, and Rem2) are small Ras-like G proteins that bind $Ca_V\beta$-subunits and profoundly inhibit all Ca_V1/Ca_V2 channels (6–8). Given their properties, RGKs straddle two worlds with respect to their impact on Ca_V1/Ca_V2 channels—they are (*i*) potentially powerful physiological regulators by virtue of their capacity to tune intracellular Ca^{2+} signals, and (*ii*) prototype genetically encoded Ca_V channel blockers with possible therapeutic and biotechnological applications (9). Consistent with important physiological roles, Rad knockout mice exhibit increased cardiac $Ca_V1.2$ currents and cardiac hypertrophy, while Gem-deficient mice display glucose intolerance and impaired glucose-stimulated insulin release. Regarding their use as potential therapeutics, expression of Gem in the atrioventricular node was effective at electrically uncoupling ventricular excitation from the fibrillating atria in a porcine model of atrial fibrillation (10). A Rem derivative engineered to selectively target and inhibit caveola-localized Ca_V channels effectively inhibited pacing-induced NFATc3-GFP translocation to the nucleus in adult feline ventricular cardiomyocytes, without affecting excitation–contraction coupling (11).

A major limitation for the use of RGKs as genetically encoded Ca_V channel blockers involves their lack of selectivity for particular Ca_V1/Ca_V2 isoforms. Rem inhibits $Ca_V1.2$ channels using multiple mechanisms including reduced channel surface density, diminished P_o, and partial immobilization of voltage sensors (12). At least one of these mechanisms (decreased P_o) involves the simultaneous association of Rem with the auxiliary $Ca_V\beta$-subunit and the plasma membrane (13, 14). This mechanism

Significance

Influx of calcium ions through surface membrane calcium channels that open in response to electrical signals is important for vital biological processes including generation of the heartbeat and nerve cell communication. Blocking such calcium channels in a tissue- and isoform-specific manner is a sought-after treatment strategy for diseases including chronic pain and Parkinson's disease. Proteins that can be expressed in cells to selectively block different calcium channel types have particular advantages over conventional small-molecule blockers. A four-member family of proteins known as RGK proteins strongly inhibit calcium channels, but do so in a non-selective manner, limiting their potential usefulness. Here we identified mutated RGK proteins that perform as isoform-selective calcium channel blockers, advancing the therapeutic potential of these proteins.

Author contributions: A.A.P., D.D.C., and H.M.C. designed research; A.A.P., D.D.C., Z.S., P.C., and H.M.C. performed research; J.S. contributed new reagents/analytic tools; A.A.P., D.D.C., Z.S., P.C., and H.M.C. analyzed data; and A.A.P., J.S., and H.M.C. wrote the paper.

The authors declare no conflict of interest.

This article is a PNAS Direct Submission.

[1]A.A.P., D.D.C., and Z.S. contributed equally to this work.

[2]To whom correspondence should be addressed. Email: hc2405@cumc.columbia.edu.

This article contains supporting information online at www.pnas.org/lookup/suppl/doi:10.1073/pnas.1811024115/-/DCSupplemental.

Published online November 5, 2018.

likely accounts for the indiscriminate nature of RGK inhibition of Ca_V1/Ca_V2 channels, since all four RGKs bind $Ca_V\beta$-subunits and the plasma membrane, and $Ca_V\beta$s are obligatory for forming functional channels. Beyond the β-binding mechanism, we previously showed that Rem can also inhibit $Ca_V1.2$ channels by directly binding to the pore-forming α_{1C}-subunit (15). Potentially, such an α_1-subunit–dependent mechanism could be exploited to develop genetically encoded Ca_V1/Ca_V2 isoform-selective inhibitors. Several outstanding questions need to be addressed to realize this potential. Does Rem inhibit other Ca_V1/Ca_V2 channels beyond $Ca_V1.2$ in a β-binding–independent manner? Do other RGKs beyond Rem inhibit Ca_V1/Ca_V2 channel isoforms in a β-binding–independent manner? Are both β-binding–dependent and β-binding–independent mechanisms of RGK inhibition of particular Ca_V1/Ca_V2 channels prevalent in native excitable cells? If so, do the two modes of inhibition display physiologically meaningful differences?

Here, focusing on four Ca_V channels ($Ca_V1.2$, $Ca_V1.3$, $Ca_V2.1$, and $Ca_V2.2$), we show that Rem uniquely blocks $Ca_V1.2$ using a β-binding–independent mechanism. Consistent with this finding, a mutant Rem that cannot bind β (Rem[R200A/L227A]) selectively blocked $Ca_V1.2$, with no effect on the closely related $Ca_V1.3$ channel. Further, Rad inhibited $Ca_V1.2$ and $Ca_V2.2$ (but not $Ca_V1.3$ or $Ca_V2.1$) channels via a β-binding–independent mechanism. Accordingly, a β-binding–deficient Rad mutant (Rad[R208A/L235A]) effectively blocked $Ca_V1.2/Ca_V2.2$, but not $Ca_V1.3/Ca_V2.1$, channels. Both Rem[R200A/L227A] and Rad[R208A/L235A] strongly inhibited endogenous $Ca_V1.2$ channels in adult ventricular cardiomyocytes. Finally, Rem[R200A/L227A] and Rad[R208A/L235A], but not Gem[R196A/V223A], inhibited HVA Ca_V channels in somatosensory dorsal root ganglion (DRG) neurons, albeit with different magnitudes reflecting their selectivity for either $Ca_V1.2$ alone or $Ca_V1.2/Ca_V2.2$, respectively. Altogether, we have exploited latent β-binding–independent inhibition of $Ca_V1.2$ and $Ca_V1.2/Ca_V2.2$ channels by Rem and Rad, respectively, to engineer genetically encoded isoform-selective Ca_V channel blockers.

Results

Differential Prevalence of β-Binding–Dependent and β-Binding–Independent Rem Inhibition Across Distinct Ca_V1/Ca_V2 Channels. We profiled β-binding–dependent (BBD) and β-binding–independent (BBI) Rem inhibition of Ca_V channels by reconstituting distinct pore-forming α_1-subunits with either wild-type β_{2a} or a mutant β_{2a} ($\beta_{2a,TM}$) that does not bind RGKs. HEK293 cells expressing α_{1C} + β_{2a} expressed robust Ba^{2+} currents (I_{Ba}) that were virtually eliminated when Rem was coexpressed (Fig. 1 *A* and *B* and *SI Appendix*, Fig. S1). Similarly, cells expressing α_{1C} + $\beta_{2a,TM}$ displayed I_{Ba} that was significantly inhibited by Rem (Fig. 1 *A* and *B* and *SI Appendix*, Fig. S1), indicating the incidence of both BBD and BBI Rem inhibition of $Ca_V1.2$ channels. These results confirm our previous report that both BBD and BBI mechanisms contribute to Rem inhibition of $Ca_V1.2$ (15). I_{Ba} influx through reconstituted $Ca_V1.3$ channels (α_{1D} + β_{2a}) was eliminated by Rem. However, $Ca_V1.3$ channels reconstituted with α_{1D} + $\beta_{2a,TM}$ were refractory to Rem (Fig. 1 *C* and *D* and *SI Appendix*, Fig. S1), indicating the absence of BBI inhibition, and revealing a fundamental difference from $Ca_V1.2$. Similar to $Ca_V1.3$, $Ca_V2.1$ (Fig. 1 *E* and *F* and *SI Appendix*, Fig. S1) and $Ca_V2.2$ (Fig. 1 *G* and *H* and *SI Appendix*, Fig. S1) channels were inhibited by Rem only when reconstituted with WT β_{2a}, but not $\beta_{2a,TM}$, a modulation profile consistent with exclusively BBD inhibition.

Engineering a $Ca_V1.2$-Selective Inhibitor from Rem. The finding that BBI Rem inhibition of I_{Ba} is a unique property of $Ca_V1.2$ suggested the possibility of engineering a $Ca_V1.2$-selective genetically encoded inhibitor by generating a Rem mutant that does not bind $Ca_V\beta$. A previous mutagenesis study identified residues in RGKs that were critical for their interaction with $Ca_V\beta$s but did not disrupt their tertiary structure, as evaluated by GTP/GDP binding assays (16). Based on these findings, we introduced two point mutations (R200A, L227A) into Rem and used FRET to evaluate the association of Rem[R200A/L227A] with $Ca_V\beta$ (Fig. 2*A*). HEK293 cells coexpressing CFP-WT Rem + YFP-β_3 displayed a significantly elevated FRET (FRET efficiency 0.188 ± 0.006, n = 127) compared with negative control cells expressing CFP-FRB + β_3-YFP (FRET efficiency 0.046 ± 0.002, n = 126) (Fig. 2*B*), consistent with well-known Rem–$Ca_V\beta$ interaction (6, 7). By comparison, cells coexpressing CFP-Rem[R200A/L227A] + β_3-YFP displayed a markedly lower FRET (FRET efficiency 0.058 ± 0.002, n = 138) that did not differ from control cells, consistent with reduced protein interaction (Fig. 2*B*). Additional insights into

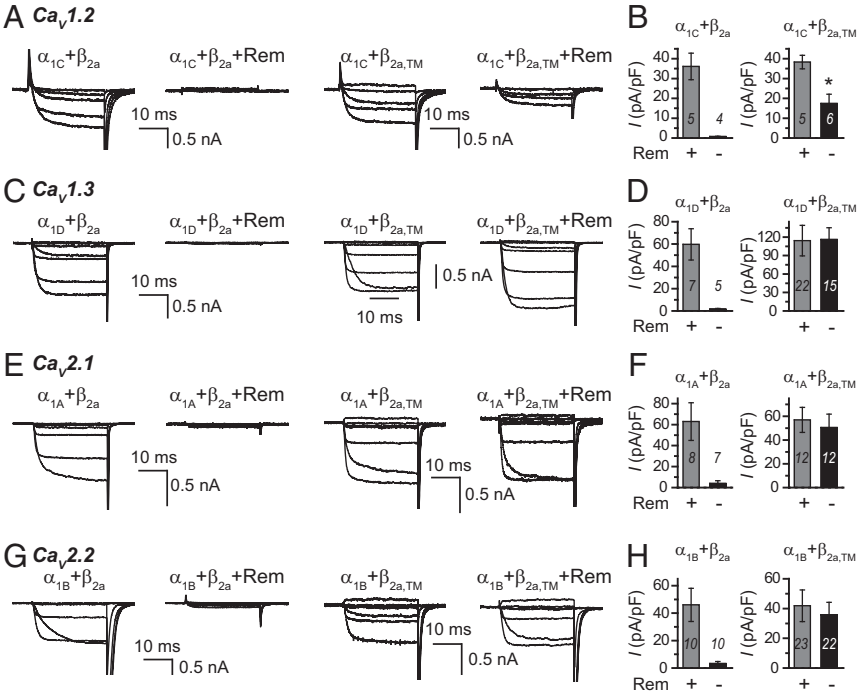

Fig. 1. Rem uniquely inhibits $Ca_V1.2$ using both β-binding–dependent and β-binding–independent mechanisms. (*A*) Exemplar $Ca_V1.2$ Ba^{2+} currents elicited from HEK293 cells expressing α_{1C} + β_{2a} ± Rem (columns 1 and 2) or α_{1C} + $\beta_{2a,TM}$ ± Rem (columns 3 and 4). Ba^{2+} currents were elicited by 25-ms test pulse depolarizations (from −50 to +100 mV in 10-mV increments) from a holding potential of −90 mV. (*B*) Population bar charts showing the impact of Rem on peak I_{Ba} from channels reconstituted with either α_{1C} + β_{2a} (*Left*) or α_{1C} + $\beta_{2a,TM}$ (*Right*). *P < 0.01, Student's unpaired t test. (*C* and *D*) Data for $Ca_V1.3$ channels reconstituted with either α_{1D} + β_{2a} ± Rem or α_{1D} + $\beta_{2a,TM}$ ± Rem, same format as *A* and *B*. (*E* and *F*) Data for $Ca_V2.1$ channels reconstituted with either α_{1A} + β_{2a} ± Rem or α_{1A} + $\beta_{2a,TM}$ ± Rem, same format as *A* and *B*. (*G* and *H*) Data for $Ca_V2.2$ channels reconstituted with either α_{1B} + β_{2a} ± Rem or α_{1B} + $\beta_{2a,TM}$ ± Rem, same format as *A* and *B*. Data are means ± SEM.

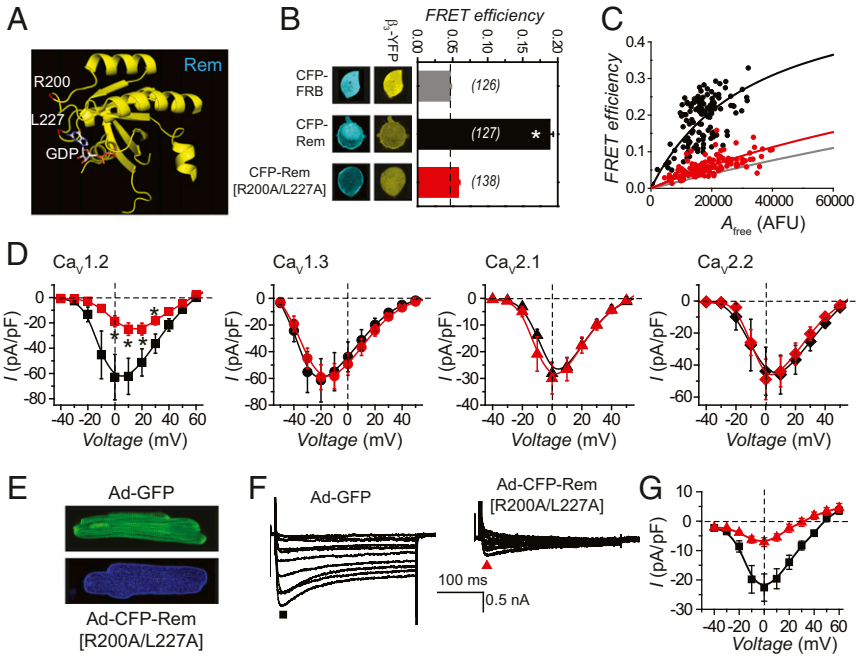

Fig. 2. Rem[R200A/L227A] does not bind $Ca_V\beta$ and selectively inhibits $Ca_V1.2$. (*A*) Crystal structure of Rem G domain with residues R200 and L227 highlighted. (*B*) FRET efficiency measurements in HEK293 cells coexpressing CFP-FRB + β_3-YFP (control), CFP-Rem + β_3-YFP, or CFP-Rem[R200A/L227A] + β_3-YFP. Data are means ± SEM. *$P < 0.01$, one-way ANOVA. (*C*) Binding-curve analyses of FRET experiments. (*D*) Population I_{peak}–*V* plots for cells expressing $\alpha_{1C} + \beta_{2a}$ (black squares; $n = 9$), $\alpha_{1C} + \beta_{2a}$ + Rem[L200A/L227A] (red squares; $n = 10$); $\alpha_{1D} + \beta_{2a}$ (black circles; $n = 11$), $\alpha_{1D} + \beta_{2a}$ + Rem[L200A/L227A] (red circles; $n = 13$); $\alpha_{1A} + \beta_{2a}$ (black triangles; $n = 10$), $\alpha_{1A} + \beta_{2a}$ + Rem[L200A/L227A] (red triangles; $n = 12$); and $\alpha_{1B} + \beta_{2a}$ (black diamonds; $n = 11$), $\alpha_{1B} + \beta_{2a}$ + Rem[L200A/L227A] (red diamonds; $n = 12$). *$P < 0.05$, Student's *t* test. (*E*) Exemplar cultured adult cardiomyocytes expressing GFP (*Top*) or CFP-Rem[L200A/L227A] (*Bottom*). (*F*) Representative Ba^{2+} currents from adult guinea pig ventricular cardiomyocytes expressing either GFP (*Left*; control) or CFP-Rem[L200A/L227A] (*Right*). (*G*) Population I_{peak}–*V* plots for cardiomyocytes expressing GFP (black squares; $n = 8$) or CFP-Rem[L200A/L227A] (red triangles; $n = 10$).

the relative affinities of Rem and Rem[R200A/L227A] for $Ca_V\beta_3$ was provided from binding analyses of FRET efficiency vs. A_{free} scatterplots (Fig. 2*C*), which indicated a fivefold decreased affinity of Rem[R200A/L227A] for $Ca_V\beta_3$ compared with WT Rem (Fig. 2*C*).

We next determined whether Rem[R200A/L227A] would function as a $Ca_V1.2$-selective inhibitor as hypothesized. Indeed, HEK293 cells coexpressing recombinant $Ca_V1.2$ ($\alpha_{1C} + \beta_{2a}$) channels and Rem[R200A/L227A] displayed significantly lower I_{Ba} compared with control cells expressing $Ca_V1.2$ alone (Fig. 2*D*; $I_{peak,10mV} = 62.3 \pm 14.3$ pA/pF, $n = 9$ for $\alpha_{1C} + \beta_{2a}$ compared with $I_{peak,10mV} = 24.9 \pm 4.9$ pA/pF, $n = 10$ for $\alpha_{1C} + \beta_{2a}$ + Rem[R200A/L227A]; $P = 0.0194$, Student's *t* test; *SI Appendix*, Fig. S2). In sharp contrast, recombinant $Ca_V1.3$, $Ca_V2.1$, and $Ca_V2.2$ were refractory to Rem[R200A/L227A] (Fig. 2*D* and *SI Appendix*, Fig. S2), consistent with this engineered protein being a $Ca_V1.2$-selective blocker. The finding that $Ca_V2.2$ is not inhibited by a β-binding–deficient Rem recapitulates a previous similar finding by Beqollari et al. (17).

To determine whether Rem[R200A/L227A] could inhibit endogenous $Ca_V1.2$ channels, we assessed its efficacy in blocking I_{Ba} conducted through native $Ca_V1.2$ channels in guinea pig ventricular cardiomyocytes. We generated adenovirus enabling robust expression of YFP-Rem[R200A/L227A] (Fig. 2*E*). Compared with control cells expressing GFP, cardiomyocytes expressing YFP-Rem[R200A/L227A] displayed a significantly reduced I_{Ba} at all test voltages (Fig. 2 *F* and *G*; $I_{peak,0mV} = 22.6 \pm 4.6$ pA/pF, $n = 8$ for GFP compared with $I_{peak,0mV} = 9.1 \pm 2.3$ pA/pF, $n = 10$, for YFP-Rem[R200A/L227A]), thus demonstrating BBI Rem inhibition of endogenous $Ca_V1.2$ channels in the heart.

Prevalence of BBD and BBI RGK Inhibition Across the Ca_V1/Ca_V2 Channel Family. We wondered whether other RGKs display BBI inhibition of Ca_V1/Ca_V2 channels that could be similarly exploited to generate selective genetically encoded inhibitors for Ca_V channels (GECCIs). We profiled the occurrence of BBD and BBI inhibition across RGKs and Ca_V1/Ca_V2 channels by assessing the impact of Gem, Rad, and Rem2 on recombinant Ca_V channels reconstituted with either WT β_{2a} or $\beta_{2a,TM}$ (Fig. 3*A* and *SI Appendix*, Fig. S3). $Ca_V1.3$ channels reconstituted with WT β_{2a} ($\alpha_{1D} + \beta_{2a}$) were uniformly inhibited by Gem, Rad, and Rem2, respectively (*SI Appendix*, Fig. S3*B*). By contrast, these three RGKs had no impact on I_{Ba} influx through $\alpha_{1D} + \beta_{2a,TM}$ channels (*SI Appendix*, Fig. S3*B*). Together, these results indicate that all RGKs inhibit $Ca_V1.3$ channels solely through a BBD mechanism. We obtained virtually identical results with reconstituted $Ca_V2.1$ channels—$\alpha_{1A} + \beta_{2a}$ channels were inhibited by Gem, Rad and Rem2, whereas $\alpha_{1A} + \beta_{2a,TM}$ channels were refractory to these RGKs (*SI Appendix*, Fig. S3*C*). Hence, $Ca_V2.1$ channels also display exclusively BBD RGK inhibition. The finding that Rem2 inhibits $Ca_V2.1$ in a solely BBD manner agrees with a previous result showing that Rem2 abolishes current through $Ca_V2.1$ channels reconstituted with WT β_4 but not a mutant β_4 lacking the capacity to bind Rem2 (18). Our finding that Gem requires binding to $Ca_V\beta$ to decrease $Ca_V2.1$ is in disagreement with a previous report that Gem binding to $Ca_V\beta_3$ was not necessary for its capacity to inhibit $Ca_V2.1$ current (19). The reasons for this discrepancy are unclear, though one possibility is the intrinsic differences between *Xenopus* oocytes (used in the previous study) and the mammalian cells used here. As expected, wild-type $Ca_V2.2$ channels ($\alpha_{1B} + \beta_{2a}$) were robustly inhibited by Gem, Rad, and Rem2, respectively. Interestingly, while channels reconstituted with $\alpha_{1B} + \beta_{2a,TM}$ were unaffected by Gem and Rem2, they were significantly inhibited by Rad (Fig. 3*B*). Therefore, Rad uniquely mediates both BBD and BBI inhibition of $Ca_V2.2$ channels. We previously reported that Rad (but not Gem or Rem2) also supports BBD and BBI inhibition of $Ca_V1.2$ (15). Together, these reports suggested that eliminating Rad binding to $Ca_V\beta$ would generate a selective inhibitor of $Ca_V1.2/Ca_V2.2$ channels.

Engineering a $Ca_V1.2$- and $Ca_V2.2$-Selective Inhibitor from Rad. Using an approach similar to the generation of Rem[R200A/L227A], we introduced equivalent mutations in Rad to create Rad[R208A/L235A]. Three-cube FRET experiments confirmed that cells expressing CFP-Rad[R208A/L235A] + YFP-β_3 showed lower FRET efficiency (0.051 ± 0.002, $n = 142$) compared with CFP-Rad + YFP-β_3 (0.123 ± 0.004, $n = 174$) (Fig. 4*B*). Binding-curve analyses indicated an eightfold decrease in affinity of CFP-Rad[R208A/L235A] for YFP-β_3 compared with CFP-Rad (Fig. 4*C*). As predicted, Rad[R208A/L235A] significantly inhibited currents through recombinant $Ca_V1.2$ ($\alpha_{1C} + \beta_{2a}$) and $Ca_V2.2$ ($\alpha_{1B} + \beta_{2a}$) channels but had no impact on either $Ca_V1.3$ ($\alpha_{1D} + \beta_{2a}$) or $Ca_V2.1$ ($\alpha_{1A} + \beta_{2a}$) channels (Fig. 4*D* and *SI Appendix*, Fig. S4). Hence, Rad[R208A/L235A] is a $Ca_V1.2/Ca_V2.2$-selective inhibitor. When expressed in guinea pig ventricular cardiomyocytes, Rad[R208A/L235A] inhibited endogenous $Ca_V1.2$ channels to almost the same extent as WT Rad (Fig. 4 *E* and *F*), revealing a strong BBI Rad inhibition of $Ca_V1.2$ in the heart. It was previously shown that Rad-inhibited

PHYSIOLOGY

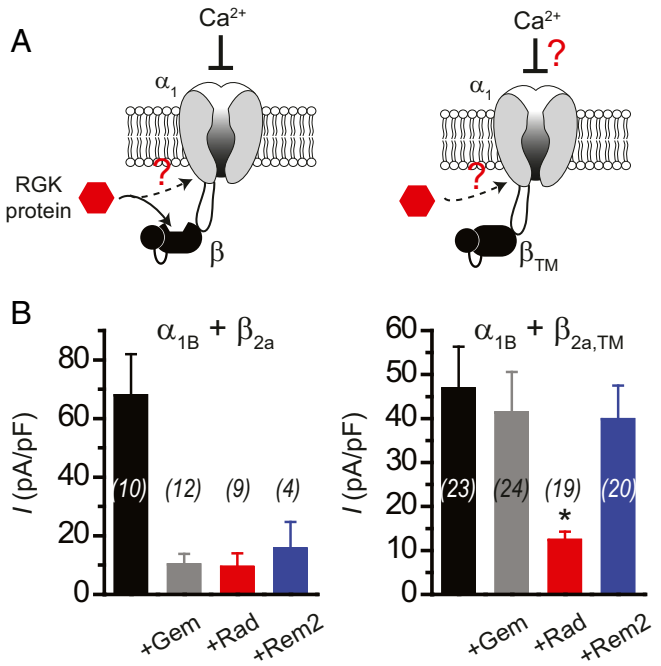

Fig. 3. Prevalence of β-binding–dependent and β-binding–independent RGK inhibition of I_{Ba} in $Ca_V2.2$ channels. (*A*) Schematic of HVA Ca_V channel pore-forming α_1-subunit binding to β_{2a} or $\beta_{2a,TM}$ with putative binding sites responsible for β-binding–dependent (solid arrow) and β-binding–independent (dashed arrows) RGK inhibition of current. (*B*) Bar charts showing impact of Gem, Rad, and Rem2 on $Ca_V2.2$ channels reconstituted with either $\alpha_{1B} + \beta_{2a}$ (*Left*) or $\alpha_{1B} + \beta_{2a,TM}$ (*Right*). Data are means ± SEM. $^*P < 0.05$ compared with control, one-way ANOVA.

$Ca_V1.2$ channels are not up-regulated by activated protein kinase A (PKA) (20). We found that I_{Ba} through ventricular $Ca_V1.2$ channels inhibited by Rad[R208A/L235A] was robustly increased by 1 μM forskolin, in sharp contrast to the lack of modulation observed with WT Rad-inhibited channels (Fig. 4 *G* and *H* and *SI Appendix*, Fig. S5). Hence, cardiac $Ca_V1.2$ channels undergoing either BBD or BBI Rad inhibition display fundamental differences in their sensitivity to PKA regulation. A caveat here is we cannot discount a contribution of $Ca_V1.2$ channels which are not bound to Rad[R208A/L235A] to the observed forskolin-induced increase in I_{Ba}. However, the finding that Rad[R208A/L235A] inhibits cardiac $Ca_V1.2$ to almost the same extent as WT Rad (Fig. 4 *E* and *F*) suggests Rad[R208A/L235A]-bound channels predominate over unbound channels, and is consistent with the interpretation that $Ca_V1.2$ channels undergoing BBI Rad inhibition are up-regulated by PKA activation.

Rem[R200A/L227A] and Rad[R208A/L235A] Inhibit HVA Ca_V Channels in Dorsal Root Ganglion Neurons. Finally, we determined the performance of Rem[R200A/L227A] and Rad[R208A/L235A] as Ca_V channel inhibitors in primary cells with a complex expression of multiple Ca_V channel types. We chose dorsal root ganglion neurons which express multiple HVA Ca_V1/Ca_V2 channels as well as low voltage-activated (LVA) $Ca_V3.2$ channels. Mouse DRG neurons express mostly $Ca_V2.1$ and $Ca_V2.2$, with a smaller contribution of $Ca_V1.2$ and $Ca_V2.3$ channels (21). We used adenoviral vectors to robustly express GFP (control) or CFP-tagged RGKs in cultured mouse DRG neurons (Fig. 5*A*). In control cells, a ramp protocol elicited two components of I_{Ba}, reflecting currents through LVA and HVA Ca_V channels, respectively. Overexpressing WT Rad essentially eliminated the HVA current component while leaving the LVA element intact (Fig. 5*B*). We further assessed the impact of various WT and mutant RGKs on the HVA Ca_V channel currents using step depolarizations. For these experiments, LVA Ca_V channel currents were eliminated by 5 μM mibefradil and a −50-mV holding potential. Control DRG neurons displayed HVA I_{Ba} currents which were dramatically reduced by WT Rad (Fig. 5 *C* and *D*; $I_{peak,-10mV} = -76.5 \pm 13.8$ pA/pF, $n = 10$ for GFP compared with $I_{peak,-10mV} = -3.5 \pm 1.3$ pA/pF, $n = 19$ for CFP-Rad; *SI Appendix*, Fig. S6). DRG neurons expressing CFP-Rad[R208A/L235A] showed a significant 62% decrease in HVA I_{Ba} compared with control (Fig. 5 *C* and *D*; $I_{peak,-10mV} = -29.8 \pm 5.8$ pA/pF, $n = 13$; *SI Appendix*, Fig. S6).

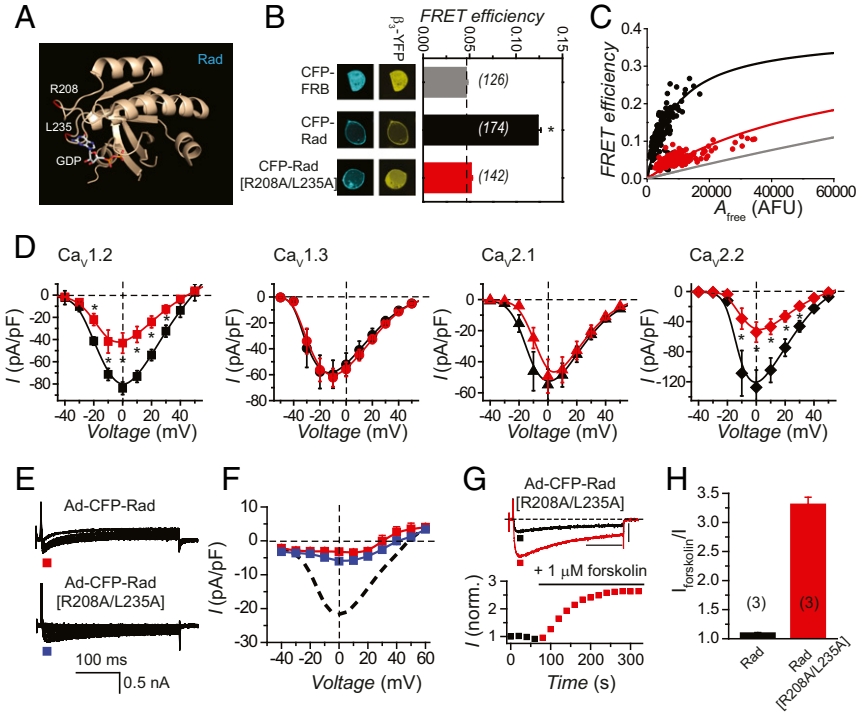

Fig. 4. Rad[R208A/L235A] does not bind $Ca_V\beta$ and selectively inhibits $Ca_V1.2$ and $Ca_V2.2$ channels. (*A*) Crystal structure of Rad G domain with residues R208 and L235 highlighted. (*B*) FRET efficiency measurements in HEK293 cells coexpressing CFP-FRB + β_3-YFP (control), CFP-Rad + β_3-YFP, or CFP-Rad[R208A/L235A] + β_3-YFP. Data are means ± SEM. $^*P < 0.01$, one-way ANOVA. (*C*) Binding-curve analyses of FRET experiments. (*D*) Population I_{peak}–*V* plots for cells expressing $\alpha_{1C} + \beta_{2a}$ (black squares; $n = 11$), $\alpha_{1C} + \beta_{2a}$ + Rad[R208A/L235A] (red squares; $n = 10$); $\alpha_{1D} + \beta_{2a}$ (black circles; $n = 10$), $\alpha_{1D} + \beta_{2a}$ + Rad[R208A/L235A] (red circles; $n = 13$); $\alpha_{1A} + \beta_{2a}$ (black triangles; $n = 10$), $\alpha_{1A} + \beta_{2a}$ + Rad[R208A/L235A] (red triangles; $n = 11$); and $\alpha_{1B} + \beta_{2a}$ (black diamonds; $n = 10$), $\alpha_{1B} + \beta_{2a}$ + Rad[R208A/L235A] (red diamonds; $n = 14$). $P < 0.05$, Student's *t* test. (*E*) Exemplar Ba^{2+} currents from cultured adult guinea pig ventricular cardiomyocytes expressing Rad (*Top*) and Rad[R208A/L235A] (*Bottom*). (*F*) Population I_{peak}–*V* for cardiomyocytes expressing either CFP-Rad (red squares; $n = 4$) or CFP-Rad[R208A/L235A] (blue squares; $n = 8$). Dotted line is mean current density for control cardiomyocytes expressing GFP, reproduced from Fig. 2*G*. (*G*) Exemplar currents (*Top*) and diary plot (*Bottom*) showing the impact of 1 μM forskolin on I_{Ba} in cardiomyocytes expressing CFP-Rad[R208A/L235A]. (*H*) Bar chart showing differential impact of forskolin in up-regulating $Ca_V1.2$ I_{Ba} in cardiomyocytes expressing CFP-Rad or CFP-Rad[R208A/L235A]. Data are means ± SEM.

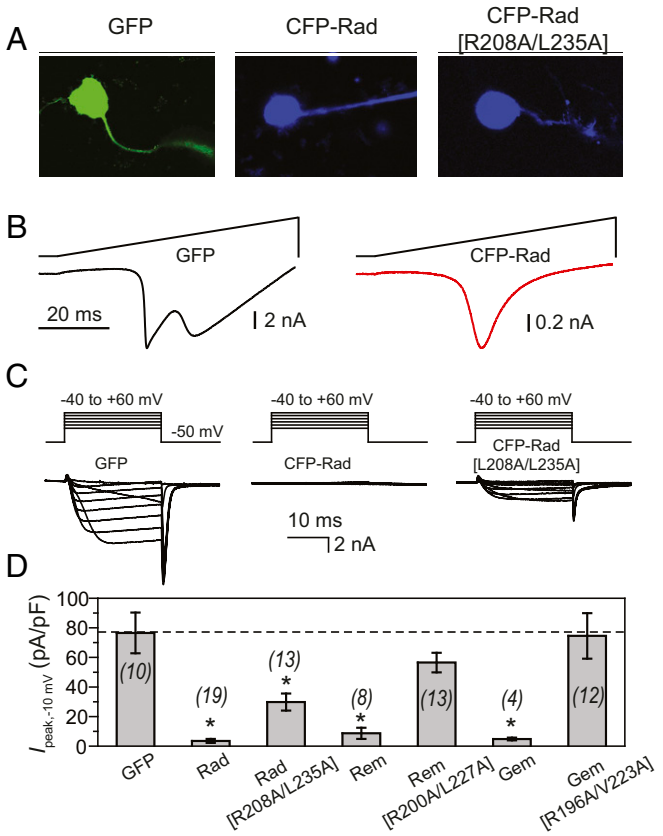

Fig. 5. Differential block of high voltage-activated Ca_V channel currents in DRG neurons by WT and mutant RGK proteins. (*A*) Representative images of cultured DRG neurons expressing GFP, CFP-Rad, or CFP-Rad[R208A/L235A]. (*B*) Exemplar I_{Ba} waveforms elicited by voltage-ramp protocols in DRG neurons expressing GFP (*Left*) or CFP-Rad (*Right*). (*C*) Exemplar family of HVA I_{Ba} from DRG neurons expressing GFP (*Left*), CFP-Rad (*Middle*), or CFP-Rad[208A/L235A] (*Right*). Currents were elicited from a holding potential of −50 mV and in the presence of 1 μM mibefradil to eliminate LVA T-type currents. (*D*) Bar chart showing the relative impact of distinct WT and β-binding–deficient mutant RGKs on HVA Ca_V1/Ca_V2 channel currents in cultured DRG neurons. Data are means ± SEM. *$P < 0.05$, one-way ANOVA and post hoc Bonferroni test.

Similar to WT Rad, DRG neurons expressing either CFP-Rem or CFP-Gem showed a dramatically reduced HVA I_{Ba} amplitude (Fig. 5*D*; $I_{peak,-10mV} = -8.7 \pm 3.8$ pA/pF, $n = 8$ for CFP-Rem, and $I_{peak,-10mV} = -4.8 \pm 0.9$ pA/pF, $n = 4$ for CFP-Gem; *SI Appendix*, Fig. S6). Expressing CFP-Rem[R200A/L227A] depressed HVA I_{Ba} by 25% compared with control (Fig. 5*D*; $I_{peak,-10mV} = -56.5 \pm 6.6$ pA/pF, $n = 13$; *SI Appendix*, Fig. S6), substantially less than the reduction observed with CFP-Rad[R208A/L235A]. By contrast, Gem[R196A/V223A] had no impact on HVA I_{Ba} in DRG neurons (Fig. 5*D*; $I_{peak,-10mV} = -74.5 \pm 15.4$ pA/pF, $n = 12$; *SI Appendix*, Fig. S6). Overall, the rank order of inhibition of HVA I_{Ba} by these mutant RGKs is consistent with the notion that CFP-Rad[R208A/L235A] inhibits both $Ca_V1.2$ and $Ca_V2.2$, CFP-Rem[R200A/L227A] inhibits only $Ca_V1.2$, and Gem[R196A/V223A] is inert against HVA Ca_V channels.

Discussion

Pharmacological blockade of distinct Ca_V1/Ca_V2 channel types is an important actual or potential therapy for many diseases, including hypertension ($Ca_V1.2$), angina ($Ca_V1.2$), cardiac arrhythmias ($Ca_V1.2$), chronic pain ($Ca_V2.2$), stroke (Ca_V2), and Parkinson's disease ($Ca_V1.3$) (1, 22, 23). Ca_V1 channels are effectively blocked by dihydropyridines, benzothiazepines, and phenylalkylamines, while Ca_V2 channels are inhibited by various animal venoms: ω-agatoxin IVA ($Ca_V2.1$), ω-conotoxins GVIA and MVIIA ($Ca_V2.2$), and SNX-482 ($Ca_V2.3$) (24). Prialt (ziconotide), a blocker of $Ca_V2.2$ derived from a marine snail conotoxin, is Food and Drug Administration-approved for the treatment of chronic pain (25). The use of small-molecule Ca_V1/Ca_V2 channel blockers is mainly limited by two factors. First, Ca_V1/Ca_V2 expression in many types of excitable cells risks prohibitive off-target effects. Second, due to a high degree of similarity among pore-forming α_1-subunits (e.g., the L-type channels, $Ca_V1.1$ to $Ca_V1.4$), currently available small-molecule blockers may not effectively distinguish between Ca_V channels of the same class. Difficulties encountered in developing $Ca_V1.3$-selective blockers as a potential treatment for Parkinson's disease exemplify these challenges (26, 27). Efficacy of such a treatment approach was suggested by reports that the reliance of substantia nigra neurons on $Ca_V1.3$ for pacemaking made them sensitive to Ca^{2+} overload and vulnerable to cell death which drives the development of Parkinson's disease (28, 29). Epidemiological studies suggest indeed some beneficial effects of L-type calcium channel (LTCC) blockers in Parkinson's disease (30). However, because the currently available LTCC blockers are not selective for $Ca_V1.3$, off-target effects (e.g., on cardiovascular $Ca_V1.2$ channels) risk serious side effects such as hypotension, significantly narrowing the therapeutic window (31).

Genetically encoded Ca_V channel blockers could offer an alternative solution without the above-mentioned drawbacks of small-molecule inhibitors. Off-target effects might be avoided by restricted expression in target tissues or defined cell populations (9, 10). RGKs are promising candidates for such an alternative treatment approach, given their potency as Ca_V channel blockers. Their potential usefulness is twofold: (*i*) as endogenous GECCIs for therapeutic or biotechnological applications, and (*ii*) as natural prototypes that can help inform strategies to design novel GECCIs for targeted applications in diseases involving excitable cells. Regarding the former, the indiscriminate nature of RGK inhibition of all Ca_V1/Ca_V2 channels represents a potential obstacle for some applications. We tested here whether selectivity for particular Ca_V1/Ca_V2 isoforms could be engineered into RGKs. Based on the intuition that the indiscriminate manner with which RGKs inhibit all Ca_V1/Ca_V2 channel types is a consequence of their binding to auxiliary $Ca_V\beta$-subunits, we mutated RGKs to eliminate their capacity of binding to $Ca_V\beta$. This simple maneuver revealed Rem[R200A/L227A] as a $Ca_V1.2$-selective blocker and Rad[R208A/L235A] as a selective inhibitor for $Ca_V1.2/Ca_V2.2$. The selectivity of Rem[R200A/L227A] for $Ca_V1.2$ over $Ca_V1.3$ is noteworthy, given that currently available small-molecule LTCC blockers do not distinguish these channels. Hence, Rem[R200A/L227A] could be a valuable tool for differentially blocking $Ca_V1.2$- and $Ca_V1.3$-mediated signaling in excitable cells, such as many types of neurons, that coexpress both channel types. Similarly, Rad[R208A/L235A] could be applied to examine $Ca_V1.2/Ca_V2.2$-dependent signaling pathways. The effectiveness of both Rem[R200A/L227A] and Rad[R208A/L235A] in blocking HVA Ca_V channels in heart cells and DRG neurons demonstrates their utility as selective GECCIs. Additionally, our experiments revealed the existence of BBI mechanisms underlying Rem and Rad inhibition of Ca_V1/Ca_V2 channels in excitable cells. This raises the question of the biological significance of BBD versus BBI Ca_V channel inhibition by RGKs. Our findings in cardiac myocytes suggest indeed functionally relevant differences between the two inhibitory mechanisms. Cardiac $Ca_V1.2$ channels are acutely up-regulated pharmacologically by agonists such as BAY K 8644 or physiological activation of PKA initiated by β-adrenergic agonists. The latter contributes to the fight-or-flight response. Rem-inhibited $Ca_V1.2$ channels in heart cells can be overridden by BAY K 8644, indicating that the blocked channels remain at the cell surface (32). However, both WT Rem- and Rad-inhibited channels are insensitive to PKA-mediated regulation (20, 32). By contrast, we found that $Ca_V1.2$ channels inhibited by either Rem[R200A/L227A] or Rad[R208A/L235A] can be robustly up-regulated by PKA. These results suggest that cardiac $Ca_V1.2$ channels inhibited by Rem or Rad through the BBD mechanism are electrically silent, while those inhibited by the BBI pathway are

PHYSIOLOGY

coincidentally activated by membrane depolarization and PKA-mediated phosphorylation. This paradigm could solve the conundrum of how a subset of $Ca_V1.2$ channels in heart cells might be reserved for signaling functions other than contraction, given that these channels are voltage-gated and the cardiac sarcolemma is subject to excitation with each heartbeat (33, 34). In this regard, it is noteworthy that GDP-bound Rem and Rad have a lower affinity for $Ca_V\beta$ than their GTP-loaded counterparts (35). We speculate that endogenous Rad toggles between BBD and BBI mechanisms to inhibit cardiac $Ca_V1.2$ channels dependent on the G domain being bound to GTP or GDP. Testing this proposition will be an interesting concept for future experiments.

Materials and Methods

Detailed methods are provided in *SI Appendix, Materials and Methods*.

Cell Culture and Transfection. Low-passage-number HEK293 cells were transiently transfected with $Ca_V\alpha$ (6 μg), $Ca_V\beta$ (4 μg), T antigen (2 μg), and RGKs (4 μg) using the calcium-phosphate precipitation method.

Primary Cell Isolation and Culture. Primary cultures of adult guinea pig heart cells and murine DRG neurons were prepared and infected with adenovirus as described (14, 36, 37). Procedures were in accordance with the guidelines of the Columbia University Animal Care and Use Committee.

Molecular Biology, Plasmids, and Adenoviral Vectors. Generation of XFP-tagged RGKs (Rad, Rem, Rem2, and Gem) and $\beta_{2a,TM}$ has been previously described (12, 15). Adenoviral vectors were generated using the AdEasy XL System (Stratagene) as previously described (38).

Electrophysiology. Whole-cell recordings were carried out at room temperature on HEK293 cells 48 to 72 h after transfection as previously described (12). Whole-cell currents were recorded from isolated ventricular myocytes as described (36, 39).

Fluorescence Resonance Energy Transfer Imaging. We used three-cube FRET to probe protein–protein interactions (35). Relative K_d and E_{max} values were calculated as previously described (35, 40).

ACKNOWLEDGMENTS. We thank Ming Chen for excellent technical support, and Dr. Shingo Kariya (Columbia University) for help with isolation of DRG neurons. This work was supported by Grants R01 HL 084332 and 1R01-GM107585 from the National Institutes of Health (to H.M.C.). A.A.P. was supported by an AHA predoctoral fellowship (13PRE13970018) and a UNCF-Merck graduate dissertation fellowship (CU11-2479). Z.S. was supported by an institutional training grant (T32HL120826). J.S. is now an employee and stock owner of Biogen; this work was completed before he joined the company. Biogen did not have a role in the design, conduct, analysis, interpretation, or funding of the research related to this work.

1. Zamponi GW, Striessnig J, Koschak A, Dolphin AC (2015) The physiology, pathology, and pharmacology of voltage-gated calcium channels and their future therapeutic potential. *Pharmacol Rev* 67:821–870.
2. Buraei Z, Yang J (2010) The β subunit of voltage-gated Ca^{2+} channels. *Physiol Rev* 90: 1461–1506.
3. Dolphin AC (2016) Voltage-gated calcium channels and their auxiliary subunits: Physiology and pathophysiology and pharmacology. *J Physiol* 594:5369–5390.
4. Ben-Johny M, Yue DT (2014) Calmodulin regulation (calmodulation) of voltage-gated calcium channels. *J Gen Physiol* 143:679–692.
5. Adams PJ, Ben-Johny M, Dick IE, Inoue T, Yue DT (2014) Apocalmodulin itself promotes ion channel opening and Ca(2+) regulation. *Cell* 159:608–622.
6. Béguin P, et al. (2001) Regulation of Ca^{2+} channel expression at the cell surface by the small G-protein kir/Gem. *Nature* 411:701–706.
7. Yang T, Colecraft HM (2013) Regulation of voltage-dependent calcium channels by RGK proteins. *Biochim Biophys Acta* 1828:1644–1654.
8. Finlin BS, Crump SM, Satin J, Andres DA (2003) Regulation of voltage-gated calcium channel activity by the Rem and Rad GTPases. *Proc Natl Acad Sci USA* 100:14469–14474.
9. Xu X, Colecraft HM (2009) Engineering proteins for custom inhibition of Ca(V) channels. *Physiology (Bethesda)* 24:210–218.
10. Murata M, Cingolani E, McDonald AD, Donahue JK, Marbán E (2004) Creation of a genetic calcium channel blocker by targeted gem gene transfer in the heart. *Circ Res* 95:398–405.
11. Makarewich CA, et al. (2012) A caveolae-targeted L-type Ca^{2+} channel antagonist inhibits hypertrophic signaling without reducing cardiac contractility. *Circ Res* 110: 669–674.
12. Yang T, Xu X, Kernan T, Wu V, Colecraft HM (2010) Rem, a member of the RGK GTPases, inhibits recombinant $Ca_V1.2$ channels using multiple mechanisms that require distinct conformations of the GTPase. *J Physiol* 588:1665–1681.
13. Puckerin AA, Chang DD, Subramanyam P, Colecraft HM (2016) Similar molecular determinants on Rem mediate two distinct modes of inhibition of $Ca_V1.2$ channels. *Channels (Austin)* 10:379–394.
14. Yang T, He LL, Chen M, Fang K, Colecraft HM (2013) Bio-inspired voltage-dependent calcium channel blockers. *Nat Commun* 4:2540.
15. Yang T, Puckerin A, Colecraft HM (2012) Distinct RGK GTPases differentially use α1- and auxiliary β-binding-dependent mechanisms to inhibit $Ca_V1.2/Ca_V2.2$ channels. *PLoS One* 7:e37079.
16. Béguin P, et al. (2007) RGK small GTP-binding proteins interact with the nucleotide kinase domain of Ca^{2+}-channel beta-subunits via an uncommon effector binding domain. *J Biol Chem* 282:11509–11520.
17. Beqollari D, Romberg CF, Filipova D, Papadopoulos S, Bannister RA (2015) Functional assessment of three Rem residues identified as critical for interactions with Ca(2+) channel β subunits. *Pflugers Arch* 467:2299–2306.
18. Xu X, Zhang F, Zamponi GW, Horne WA (2015) Solution NMR and calorimetric analysis of Rem2 binding to the Ca^{2+} channel β4 subunit: A low affinity interaction is required for inhibition of Cav2.1 Ca^{2+} currents. *FASEB J* 29:1794–1804.
19. Fan M, Buraei Z, Luo HR, Levenson-Palmer R, Yang J (2010) Direct inhibition of P/Q-type voltage-gated Ca^{2+} channels by Gem does not require a direct Gem/Ca_vbeta interaction. *Proc Natl Acad Sci USA* 107:14887–14892.
20. Wang G, et al. (2010) Rad as a novel regulator of excitation-contraction coupling and beta-adrenergic signaling in heart. *Circ Res* 106:317–327.
21. Murali SS, et al. (2015) High-voltage-activated calcium current subtypes in mouse DRG neurons adapt in a subpopulation-specific manner after nerve injury. *J Neurophysiol* 113:1511–1519.
22. Triggle DJ (2007) Calcium channel antagonists: Clinical uses—Past, present and future. *Biochem Pharmacol* 74:1–9.
23. Valentino K, et al. (1993) A selective N-type calcium channel antagonist protects against neuronal loss after global cerebral ischemia. *Proc Natl Acad Sci USA* 90: 7894–7897.
24. Simms BA, Zamponi GW (2014) Neuronal voltage-gated calcium channels: Structure, function, and dysfunction. *Neuron* 82:24–45.
25. Wermeling DP (2005) Ziconotide, an intrathecally administered N-type calcium channel antagonist for the treatment of chronic pain. *Pharmacotherapy* 25:1084–1094.
26. Kang S, et al. (2012) $Ca_V1.3$-selective L-type calcium channel antagonists as potential new therapeutics for Parkinson's disease. *Nat Commun* 3:1146.
27. Huang H, et al. (2014) Modest $Ca_V1.342$-selective inhibition by compound 8 is β-subunit dependent. *Nat Commun* 5:4481.
28. Surmeier DJ, Schumacker PT (2013) Calcium, bioenergetics, and neuronal vulnerability in Parkinson's disease. *J Biol Chem* 288:10736–10741.
29. Guzman JN, et al. (2010) Oxidant stress evoked by pacemaking in dopaminergic neurons is attenuated by DJ-1. *Nature* 468:696–700.
30. Ritz B, et al. (2010) L-type calcium channel blockers and Parkinson disease in Denmark. *Ann Neurol* 67:600–606.
31. Simuni T, et al. (2010) Tolerability of isradipine in early Parkinson's disease: A pilot dose escalation study. *Mov Disord* 25:2863–2866.
32. Xu X, Marx SO, Colecraft HM (2010) Molecular mechanisms, and selective pharmacological rescue, of Rem-inhibited $Ca_V1.2$ channels in heart. *Circ Res* 107:620–630.
33. Shaw RM, Colecraft HM (2013) L-type calcium channel targeting and local signalling in cardiac myocytes. *Cardiovasc Res* 98:177–186.
34. Molkentin JD (2006) Dichotomy of Ca^{2+} in the heart: Contraction versus intracellular signaling. *J Clin Invest* 116:623–626.
35. Chang DD, Colecraft HM (2015) Rad and Rem are non-canonical G-proteins with respect to the regulatory role of guanine nucleotide binding in Ca(V)1.2 channel regulation. *J Physiol* 593:5075–5090.
36. Miriyala J, Nguyen T, Yue DT, Colecraft HM (2008) Role of Ca_Vbeta subunits, and lack of functional reserve, in protein kinase A modulation of cardiac $Ca_V1.2$ channels. *Circ Res* 102:e54–e64.
37. Albuquerque C, Joseph DJ, Choudhury P, MacDermott AB (2009) Dissection, plating, and maintenance of dorsal root ganglion neurons for monoculture and for coculture with dorsal horn neurons. *Cold Spring Harb Protoc* 2009:pdb.prot5275.
38. Subramanyam P, et al. (2013) Manipulating L-type calcium channels in cardiomyocytes using split-intein protein transsplicing. *Proc Natl Acad Sci USA* 110:15461–15466.
39. Colecraft HM, et al. (2002) Novel functional properties of Ca(2+) channel beta subunits revealed by their expression in adult rat heart cells. *J Physiol* 541:435–452.
40. Chen H, Puhl HL, III, Ikeda SR (2007) Estimating protein-protein interaction affinity in living cells using quantitative Förster resonance energy transfer measurements. *J Biomed Opt* 12:054011.